JACS
JOURNAL OF THE AMERICAN CHEMICAL SOCIETY

Subscriber access provided by ISTANBUL TEKNIK UNIV

Article

Analysis of Chemical Shift Changes Reveals the Binding Modes of Isoindolinone Inhibitors of the MDM2-p53 Interaction

Christiane Riedinger, Jane A. Endicott, Stuart J. Kemp, Lynette A. Smyth, Anna Watson, Eric Valeur, Bernard T. Golding, Roger J. Griffin, Ian R. Hardcastle, Martin E. Noble, and James M. McDonnell

J. Am. Chem. Soc., **2008**, 130 (47), 16038-16044 • DOI: 10.1021/ja8062088 • Publication Date (Web): 30 October 2008

Downloaded from http://pubs.acs.org on February 8, 2009

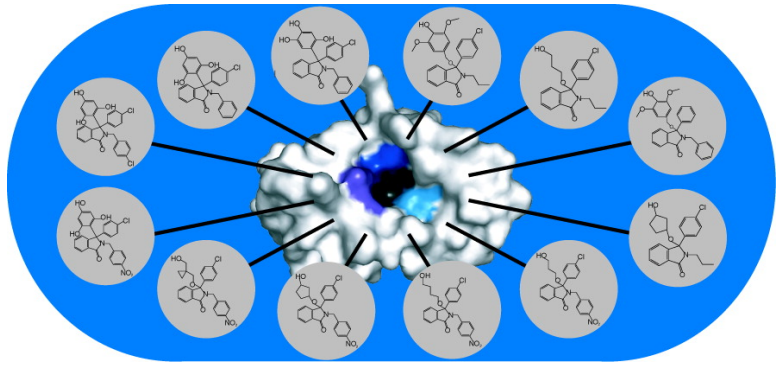

More About This Article

Additional resources and features associated with this article are available within the HTML version:

- Supporting Information
- Access to high resolution figures
- Links to articles and content related to this article
- Copyright permission to reproduce figures and/or text from this article

View the Full Text HTML

ACS Publications
High quality. High impact.

Journal of the American Chemical Society is published by the American Chemical Society. 1155 Sixteenth Street N.W., Washington, DC 20036

J|A|C|S
ARTICLES

Published on Web 10/30/2008

Analysis of Chemical Shift Changes Reveals the Binding Modes of Isoindolinone Inhibitors of the MDM2-p53 Interaction

Christiane Riedinger,[†] Jane A. Endicott,[†] Stuart J. Kemp,[‡] Lynette A. Smyth,[‡] Anna Watson,[‡] Eric Valeur,[‡] Bernard T. Golding,[‡] Roger J. Griffin,[‡] Ian R. Hardcastle,[‡] Martin E. Noble,[†] and James M. McDonnell*,[†]

Laboratory of Molecular Biophysics, Department of Biochemistry, University of Oxford, South Parks Road, Oxford, OX1 3QU, U.K., and Northern Institute for Cancer Research, Bedson Building, University of Newcastle, NE1 4RW, U.K.

Received August 7, 2008; E-mail: james.mcdonnell@bioch.ox.ac.uk

Abstract: In this study we present a method for defining the binding modes of a set of structurally related isoindolinone inhibitors of the MDM2-p53 interaction. This approach derives the location and orientation of isoindolinone binding, based on an analysis of the patterns of magnitude and direction of chemical shift perturbations for a series of inhibitors of the MDM2-p53 interaction. The MDM2-p53 complex is an attractive target for therapeutic intervention in cancer cells with intact tumor suppressor p53, as it offers the possibility of releasing p53 by blocking the MDM2-p53 binding site with a small molecule antagonist to promote apoptosis. Isoindolinones are a novel class of MDM2-antagonists of moderate affinity, which still require the development of more potent candidates for clinical applications. As the applicability of conventional structural methods to this system is limited by a number of fundamental factors, the exploitation of the information contained in chemical shift perturbations has offered a useful route to obtaining structural information to guide the development of more potent compounds. For a set of 12 structurally related isoindolinones, the data suggests 4 different orientations of binding, caused by subtle changes in the chemical structure of the inhibitors.

Introduction

The transcription factor p53 is the cell's major tumor suppressor and is found to be mutated in more than 50% of cancers.[1,2] In malignant cells with an intact p53 gene, p53 function is prohibited by other mechanisms, such as the overexpression of its main antagonist, the ubiquitin ligase MDM2.[3] MDM2 and p53 are mutually regulated through an autoregulatory feedback loop:[4,5] P53 initiates transcription of MDM2, which in turn binds to p53, blocking its activity as a transcription factor and targeting p53 for degradation.[6−9] Disruption of the MDM2-p53 interaction is an attractive target for drug design as MDM2 antagonists restore wild-type p53 function and trigger apoptosis. Furthermore, the molecular details of MDM2-p53 binding present one of the few cases in which protein−protein interactions have been shown to be amenable to inhibition by small molecules.[10]

A number of high-affinity small-molecule inhibitors of the MDM2-p53 interaction have been presented in the literature: the Nutlins, derived from an imidazole scaffold, were first reported in 2004.[11] The most potent Nutlin inhibitor, Nutlin3a, has been shown to selectively activate p53 and induce apoptosis in selected cancer cell lines.[12] In 2005, a benzodiazepine-derived MDM2-antagonist was reported and later shown to suppress human tumor cell proliferation.[13,14] A third class of spiroxindole-based compounds was very recently shown to completely inhibit tumor growth in tumor xenograft tissues.[15]

In 2005, isoindolinone-based inhibitors of the MDM2-p53 interaction were first presented, identified from *in silico* screening.[16] Initial compounds displayed promising biological activity in an ELISA competition assay, which determined the IC_{50} values with respect to a p53 reporter peptide.[16] Furthermore, isoindolinones were shown to induce dose-dependent p53-

[†] University of Oxford.
[‡] University of Newcastle.

(1) Levine, A. J. *Cell* **1997**, *88*, 323–31.
(2) Hainaut, P.; Hollstein, M. *Adv. Cancer Res.* **2000**, *77*, 81–137.
(3) Momand, J.; Jung, D.; Wilczynski, S.; Niland, J. *Nucleic Acids Res.* **1998**, *26*, 3453–9.
(4) Picksley, S. M.; Lane, D. P. *Bioessays* **1993**, *15*, 689–90.
(5) Wu, X.; Bayle, J. H.; Olson, D.; Levine, A. J. *Genes Dev.* **1993**, *7*, 1126–32.
(6) Barak, Y.; Juven, T.; Haffner, R.; Oren, M. *Embo J* **1993**, *12*, 461–8.
(7) Chen, J.; Marechal, V.; Levine, A. J. *Mol. Cell. Biol.* **1993**, *13*, 4107–14.
(8) Momand, J.; Zambetti, G. P.; Olson, D. C.; George, D.; Levine, A. J. *Cell* **1992**, *69*, 1237–45.
(9) Honda, R.; Tanaka, H.; Yasuda, H. *FEBS Lett.* **1997**, *420*, 25–7.
(10) Kussie, P. H.; Gorina, S.; Marechal, V.; Elenbaas, B.; Moreau, J.; Levine, A. J.; Pavletich, N. P. *Science* **1996**, *274*, 948–53.
(11) Vassilev, L. T.; Vu, B. T.; Graves, B.; Carvajal, D.; Podlaski, F.; Filipovic, Z.; Kong, N.; Kammlott, U.; Lukacs, C.; Klein, C.; Fotouhi, N.; Liu, E. A. *Science* **2004**, *303*, 844–8.
(12) Gu, L.; Zhu, N.; Findley, H. W.; Zhou, M. *Leukemia* **2008**, *22*, 730–9.
(13) Grasberger, J.; et al. *Med. Chem.* **2005**, *48*, 909–12.
(14) Koblish, H. K.; et al. *Mol. Cancer Ther.* **2006**, *5*, 160–9.
(15) Shangary, S.; et al. *Proc. Natl. Acad. Sci. U.S.A.* **2008**, *105*, 3933–8.
(16) Hardcastle, I. R.; et al. *Bioorg. Med. Chem. Lett.* **2005**, *15*, 1515–20.

10.1021/ja8062088 CCC: $40.75 © **2008 American Chemical Society**

dependent gene transcription in MDM2-amplified SJSA human sarcoma cell lines.

Initial generations of isoindolinones bound MDM2 with only micromolar IC_{50}, hence much higher potency is required for successful inhibition *in vivo*. Unfortunately, attempts to significantly improve potency through a combined approach of combinatorial chemistry and molecular docking were hampered by a lack of definite structural information about the inhibitor binding mode. Standard SAR analysis suggested that multiple binding orientations may exist and that the introduction of new functional groups into the isoindolinone scaffold might reorient the inhibitor in the binding pocket.[17] In this situation, the availability of structural information of MDM2 in complex with isoindolinones is crucial, as it allows explanation of the SAR data, but also provides the basis for rational design of compounds with increased potency.

Unfortunately, obtaining conventional structural information for protein-inhibitor complexes of moderate affinities as observed for isoindolinones poses a dilemma: the stability of the complex can preclude crystallographic analysis, especially when dealing with flexible proteins and moderately soluble ligands of weak affinities. Moreover, NMR structure determination is challenging due to the difficulty of achieving saturation at the required protein concentration. Furthermore, low micromolar affinity for the target is often accompanied by line-broadening caused by intermediate exchange, which renders the measurement of NOEs as structural restraints very difficult unless special methods are employed to build up measurable NOEs.[18] Finally, it is still a major challenge in computational docking to distinguish the native binding mode from a number of inaccurate poses based on the energy scoring function. In the case of the isoindolinones, this is particularly challenging, as there are a large number of possible orientations. Furthermore, computational docking is less successful when dealing with hydrophobic interactions such as ligand-binding to MDM2 where only few hydrogen bonds are involved.[10]

NMR chemical shift perturbations have often been used to determine the location of ligand binding.[19] Unfortunately, information about the orientation of the ligand cannot be extracted from this type of analysis alone. It has, however, been possible to determine binding modes from a comparison between predicted chemical shift perturbations for a number of computationally predicted poses and the experimentally observed values.[20] This method was shown to be more successful than computational docking alone.[21] A similar approach is applied in "protein−ligand NOE matching", where predicted and observed protein−ligand NOE patterns are compared to derive the true binding pose.[22] There are, however, very few examples in the literature that attempt to directly evaluate chemical shift perturbations to derive information about ligand binding. The key to such an approach lies in the comparison of shifts induced by a number of structurally related ligands. Medek et al. have presented one such case where the perturbations caused by three chemical analogs of two parent ligands were subtracted to obtain the location of the structurally dissimilar part of the ligands.[23] Calculating the differential of chemical shift perturbations however requires that the ligands bind in a similar orientation.

In this study, we present a simple method to determine the orientation of a ligand in a protein binding-pocket through analysis of magnitude and direction of amide chemical shift perturbations for a series of structurally similar ligands. By comparing the chemical shift changes induced by structurally closely related compounds, it is possible to map the location of the structurally dissimilar moiety of the ligands to the surface area experiencing a difference in chemical shift change. This approach seeks to maximize the information derivable from ligand-induced chemical shift perturbations. We have tested 12 isoindolinone inhibitors of the MDM2-p53 interaction, divisible into three groups of compounds, which differ only in one R-group attached to the main scaffold (Figure 1). Detailed analysis of the chemical shift changes induced in each residue forming the surface of MDM2's hydrophobic pocket revealed four inhibitor binding orientations, induced by subtle differences in the ligand's chemical structure.

Experimental Section

Protein Expression and Purification. NMR titrations were carried out with a 12 kDa construct of MDM2, comprising residues 17−125, expressed from pGEX-6P1 in BL21(DE3) cells as a GST fusion. Cell cultures were supplemented with 50 μg/mL ampicillin for plasmid selection. 500 mL cultures of BL21-DE3 cells were grown to an OD_{600} of 0.6−0.8 and induced with 0.2 mM IPTG. Protein expression was maintained for 3−6 h at 25 °C. The cells were harvested at 40 000 rpm (13 000 g) and 4 °C for 20 min and the cell pellets were resuspended on ice in 20−40 mL resuspension buffer (200 mM NaCl, 50 mM Na_2HPO_4, pH 6.5, 0.01% (v/v) α-monothioglycerol, 4× Sigma Inhibitor Cocktail) per liter of culture. The cell solution was flash frozen in liquid nitrogen and stored at −80 °C. Each equivalent of 500 mL culture was lysed on ice for a total time of 3 min carried out in 9 cycles of 20 s sonication followed by 20 s of rest. Sonicated samples were centrifuged in a Beckman L8−70 M ultracentrifuge and 70Ti rotor at 38 000 rpm at 4 °C for 30 min. The cell lysate was loaded onto a gravity flow glutathione Sepharose column (GE Healthcare) containing 4 mL of resin equilibrated in PBS buffer (200 mM NaCl, 50 mM Na_2HPO_4, pH 6.5, 0.01% (v/v) α-monothioglycerol, 0.01% sodium azide). The column was washed with 50 mL of PBS buffer and the protein was eluted in 30 mL of PBS buffer supplemented with 20 mM glutathione (pH 6.5). The protein was cleaved overnight with 1/20 (w/w) 3C precision protease (prepared in house as a GST-fusion) and then further purified by size exclusion chromatography using a HighLoad 26/60 Superdex 200 column (GE Healthcare), equilibrated with PBS buffer.

Inhibitor Synthesis. Inhibitors Ia, Ia″ and Ib were synthesized as described by Hardcastle et al.[24] Inhibitors Ic, as well as inhibitors of group II and III were synthesized as described in the Supporting Information.

NMR Titrations. Pure ^{15}N-labeled MDM2 was concentrated to 150−300 μM in PBS buffer and supplemented with 5% deuterated DMSO, to increase compound solubility, and 5% D_2O, used for deuterium locking. Small molecule-ligands were dissolved in deuterated DMSO to a final concentration of 40 mM. The peptide stock was prepared by dissolving lyophilized $p53_{17-29}$ in PBS buffer to a final concentration of 20 mM. Ligands were added in increments of 25% total protein concentration to a maximum ratio of ligand to protein of 2:1. For each titration point, ^{1}H,^{15}N-HSQC spectra were acquired at 500, 600 and 750 MHz on home-built

(17) Hardcastle, I. R.; et al. *J. Med. Chem.* **2006**, *49*, 6209–21.
(18) Reibarkh, M.; Malia, T. J.; Hopkins, B. T.; Wagner, G. *J. Biomol. NMR* **2006**, *36*, 1–11.
(19) Zuiderweg, E. R. *Biochemistry* **2002**, *41*, 1–7.
(20) Wang, B.; Raha, K.; Merz, K. M., Jr. *J. Am. Chem. Soc.* **2004**, *126*, 11430–1.
(21) Wang, B.; Westerhoff, L. M.; Merz, K. M., Jr. *J. Med. Chem.* **2007**, *50*, 5128–34.
(22) Constantine, K. L.; Davis, M. E.; Metzler, W. J.; Mueller, L.; Claus, B. L. *J. Am. Chem. Soc.* **2006**, *128*, 7252–63.
(23) Medek, A.; Hajduk, P. J.; Mack, J.; Fesik, S. W. *J. Am. Chem. Soc.* **2000**, *122*, 1241–42.
(24) Hardcastle, I. R.; et al. *J. Med. Chem.* **2006**, *49*, 6209–6221.

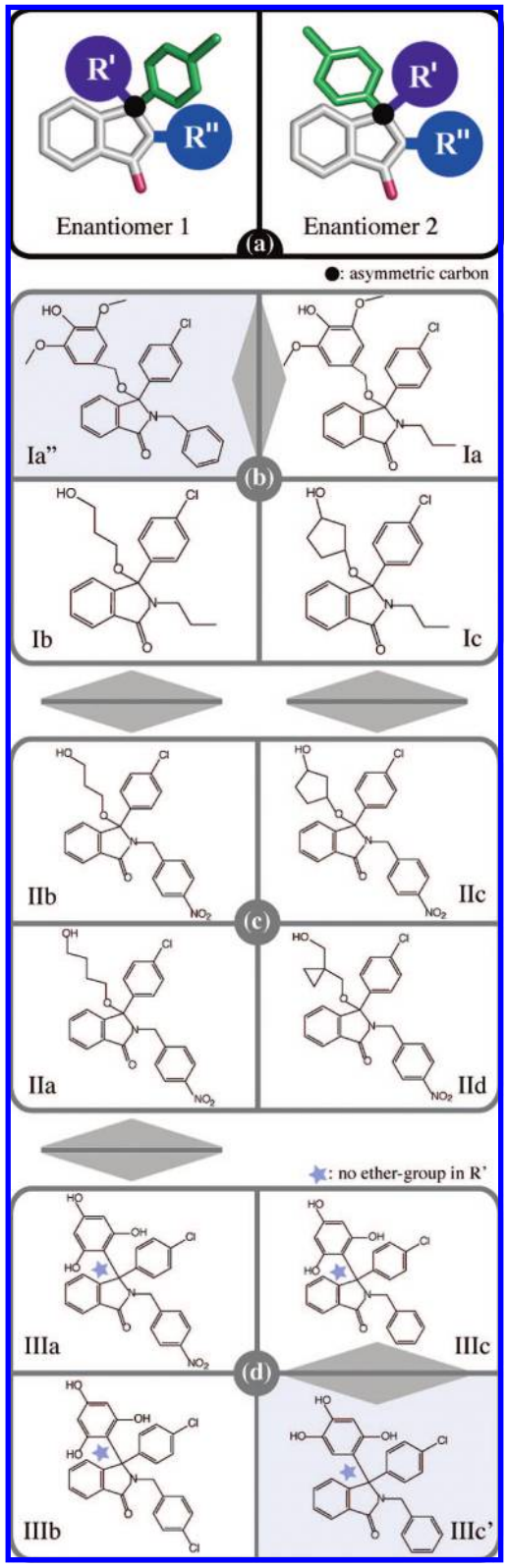

Figure 1. Isoindolinone-based inhibitors of the MDM2-p53 interaction, depicting the main scaffold, nomenclature of enantiomers and chemical structure of inhibitors tested. (a) To maintain a consistent nomenclature for all inhibitors tested in this study, the two enantiomers existing for each compound were defined according to the configuration of the para-chlorophenyl group with respect to the isoindolinone unit. IUPAC nomenclature for each inhibitor can be found in the Supporting Information. (b−d) Group I and II differ structurally in R′, group III in R″. Pairs of inhibitors differing in one R-group are indicated by double-sided arrows.

OMEGA spectrometers. Acquisition times in the direct and indirect dimensions were 102.4 and 25 ms, respectively. The spectral width in the nitrogen dimension was 25 ppm, centered at 117.25 ppm. Data was processed using a 70° shifted sine-bell window function and zero-filling to three times the number of points using NMRPipe.[25] The final digital resolution of all spectra was 0.005 ppm/point in both direct and indirect dimensions. Fourteen titrations were carried out in total using 12 isoindolinones, Nutlin3 and a p53-peptide comprising residues 17−29.

MDM2 Backbone Assignments. Pure $^{13}C,^{15}N$-labeled $MDM2_{17-125}$ was prepared at a concentration of 150 μM in PBS buffer supplemented with 5% D_2O for deuterium locking, and 10% D-glycerol for protein stabilization. Due to the low protein concentration, only experiments with high inherent signal such as the HNCA and CBCA(CO)NH could be acquired. Two identical data sets were acquired with *apo*-MDM2 and $p53_{17-29}$-bound MDM2 at 2:1 saturation. Experiments were performed at 20 °C using a 500 MHz spectrometer (11.7 T) equipped with a cryogenic probe-head and commercial console. The acquisition time in the direct dimension was 80 ms, 24 ms in the nitrogen dimension and 15 ms in the carbon dimension. A 70° shifted sine-bell window function was applied in each dimension and data was zero-filled to three times the number of points using NMRPipe.[25] Data were referenced to DSS (2,2-Dimethyl-2-silapentane-5-sulfonate sodium salt) as an internal standard. Final spectra were analyzed using NMRView.[26] Full backbone assignments were obtained for all residues situated in well-ordered parts of the protein and are contained in the Supporting Information. The chemical shifts for $MDM2_{17-125}$ are available from the BioMagResBank (BMRB) database under accession number 15945. Previous published assignments of $MDM2_{1-118}$ were used to validate the results of this assignment process.[27]

Chemical Shift Changes. The combined chemical shift change was calculated as follows:

$$\Delta\delta(^1H, ^{15}N) = \sqrt{\Delta\delta(^1H)^2 + 0.04 \cdot \Delta\delta(^{15}N)^2} \qquad (1)$$

Shift average and standard deviation were determined to develop a rational categorization of chemical shifts, rather than choosing arbitrary values to define small, medium and large perturbations. A large shift was defined as a value higher than the average of all combined shifts plus one standard deviation. A small shift was defined as below the average shift, while intermediate shifts lay between average and large shifts. The combined chemical shift changes for each ligand were evaluated according to these criteria. Colors were assigned to each category and then visualized by mapping onto the $MDM2_{17-125}$ structure.

Manual Docking. Twenty-four isoindolinone structures were generated with the program Chemdraw (CambridgeSoft, Cambridge, MA) and then minimized with the program Corina (Molecular Networks GmbH, Erlangen, Germany). These compounds were then docked manually into the structure of MDM2 (PDB accession code 1YCR) using the program PyMOL, according to the restraints derived from the chemical shift analysis.[10,28]

Computational Docking. Based on the NMR data, we were able to suggest a single binding model for most stereoisomers of the twelve isoindolinones tested. Assuming that only one enantiomer binds to MDM2 with a high affinity, it now remained to be determined which of the two possible binding modes per compound is the preferred one. We next performed *ab initio* docking using

(25) Delaglio, F.; Grzesiek, S.; Vuister, G. W.; Zhu, G.; Pfeifer, J.; Bax, A. *J Biomol NMR* **1995**, *6*, 277–93.
(26) Johnson, B. A.; Blevins, R. A. *J. Biomol. NMR* **1994**, 603–614.
(27) Stoll, R.; Renner, C.; Muhlhahn, P.; Hansen, S.; Schumacher, R.; Hesse, F.; Kaluza, B.; Engh, R. A.; Voelter, W.; Holak, T. A. *J. Biomol. NMR* **2000**, *17*, 91–2.
(28) DeLano, W. L. The PyMOL Molecular Graphics System (2002) on the World Wide Web http://www.pymol.org. The PyMOL program was used to generate Figures 2 and 3b−d.

the program GOLD, to predict preferences in binding to MDM2 for the isoindolinone enantiomers.[29] The structures of all 12 isoindolinones with both enantiomers were generated in CS ChemDraw Ultra (CambridgeSoft) and minimized using the program Corina (Molecular Networks). The binding pocket was loosely defined as the vicinity of residue Ile61 at the surface of MDM2, roughly corresponding to the Phe19 subpocket. The molecular docking runs were performed for all 24 compounds. The simulations were terminated automatically as soon as several docking solutions were identical. The solutions were inspected visually and classified according to the different binding orientations present. These solutions were then compared to the results obtained from manual docking.

Results

To enable a comparison of chemical shifts induced by isoindolinones, the chemical structures of the ligands must be rationalized. Inhibitors were grouped into pairs or small groups of compounds that differ in only one element of their chemical structure. Isoindolinone inhibitors consist of a 3-bladed propeller-like structure with the isoindolinone moiety in its center, with a para-chlorophenole moiety attached to position 2 and two R groups (R′ and R″) attached to position 3 of the isoindolinone system (Figure 1). The set of compounds analyzed in this study could therefore easily be divided into groups of inhibitors differing in only one structural element, either R′ or R″.

As shown in Figure 1, group I contains inhibitors Ia, Ia″, Ib and Ic which differ in the functional group R′. Inhibitors Ia and Ia″ only differ in R″ which is, respectively, a benzyl or *n*-propyl group for Ia″ and Ia. Inhibitors a, b, c and d within group II all have a para-nitrobenzyl group at R″ but differ in their R′ groups. Compound IIIa could also be a member of group II, but has been included in group III because its R′ functional group lacks an ether function. Group III inhibitors have identical R′ groups, but differ in the substituents of the benzyl-group R″. Compound IIIc′ is very closely related to IIIc in that the three hydroxy-substituents of the phenyl-group (R′) are located at the 2,4,5- and 2,4,6-positions, respectively. Compounds IIIc and IIIc′ have not been grouped with inhibitor Ia″, because Ia″, unlike the group III compounds, contains an ether-bridge in R′. The ether-group has a dramatic effect on the possible conformations that the isoindolinones can adopt. In the absence of this functional group, the molecules are very rigid, as only the R″ group can provide significant rotational freedom.

Predicting isoindolinone-binding is particularly challenging, since the architecture of the active site and the isoindolinone scaffold permit 12 possible orientations of binding for each compound. This number results from the main chemical scaffold of isoindolinones (Figure 1), which dock into a binding-site consisting of four subpockets (Figure 2). Since no enantioselective synthesis is currently available for isoindolinones, inhibitors are synthesized as a mixture of the two main enantiomers. This increases the total number of possible orientations to 24. For each inhibitor there will be one preferred binding mode, which we seek to determine here.

The analysis of the direction of chemical shift changes was done using so-called "per-residue plots" (Figure 3). These plots combine the information contained in all titration spectra at saturation, relative to the peak-position in the apo-state. The location of the peaks with respect to the origin of the coordinate system represents the chemical shift changes induced by each of the ligands for each residue of MDM2. A total of 38 residues near the interaction site, which were most likely to be affected by ligand-binding, were included in the analysis, namely helix α2 (residues 50−63), residues Y67 to V75, helix α1′ (residues 82−86) and residues 91−106, comprising helix α2′.

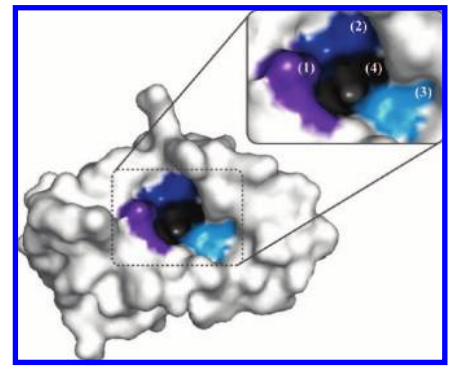

Figure 2. Surface representation of MDM2 (1YCR), highlighting the four subpockets of the p53-binding site. (1) Trp23 of p53 forms a hydrogen bond with residue Leu54, part of a shallow pocket highlighted in purple. (2) Subpocket comprising residues Ile99 and Ile103, binding to Leu26 of p53, is shown in blue. (3) Pocket around residue Ile61, accommodating Phe19 of p53 is shown in light blue. (4) Deep pocket accepting the Trp23-side chain of p53 is highlighted in gray.

A cluster analysis was then performed for each per-residue plot, by categorizing peaks according to their distribution in the bound state. Closely clustered peaks were considered as similar in terms of the effects caused by inhibitor binding on the amino acid of interest. Unclustered peaks in the bound states suggest a change in the ligand binding orientation at this site. This analysis was repeated for different subgroups of inhibitors, that is, all isoindolinones, inhibitors within groups I, II and III, pairs Ia and Ia″, pair IIa and IIIa and pair IIIc and IIIc′, inhibitor IIIa versus group II, group I versus group B, all inhibitors within group III, and finally inhibitor IIIa versus Nutlin3. Classification was not attempted when more than 50% of the subgroup to be analyzed experienced line-broadening for the amino acid in question.

The results from the cluster analyses were plotted onto the crystal structure of $MDM2_{17-125}$ (1YCR) to highlight surface patches experiencing similar/different changes in their chemical environment. Since the subgroups defined in each cluster-analysis contain inhibitors that differ in only one structural moiety, the surface areas with different effects were now correlated to the location of the structurally dissimilar part of the ligand. Once the location of these R-groups was identified, the group of inhibitors of interest was docked manually into the 1YCR structure of MDM2, to determine which orientations in agreement with the NMR data are possible in three-dimensional space. The manual docking was carried out with PyMOL. Using this approach, we were able to narrow down the number of possible binding modes to one single solution for each stereoisomer of all inhibitors except enantiomers 2 of group II, for which there were two final solutions (Figure 4).

The binding modes obtained in this way were then compared to the ones obtained from computational docking, using the program GOLD.[29] For the 24 structures (twelve inhibitors each with two enantiomers) docked into the 1YCR structure of MDM2, GOLD predicted over 150 solutions, which were summarized according to the different orientations of binding observed. For each enantiomer, the NMR derived binding mode was compared to the predicted models obtained from GOLD

(29) Verdonk, M. L.; Cole, J. C.; Hartshorn, M. J.; Murray, C. W.; Taylor, R. D. *Proteins* **2003**, *52*, 609–23.

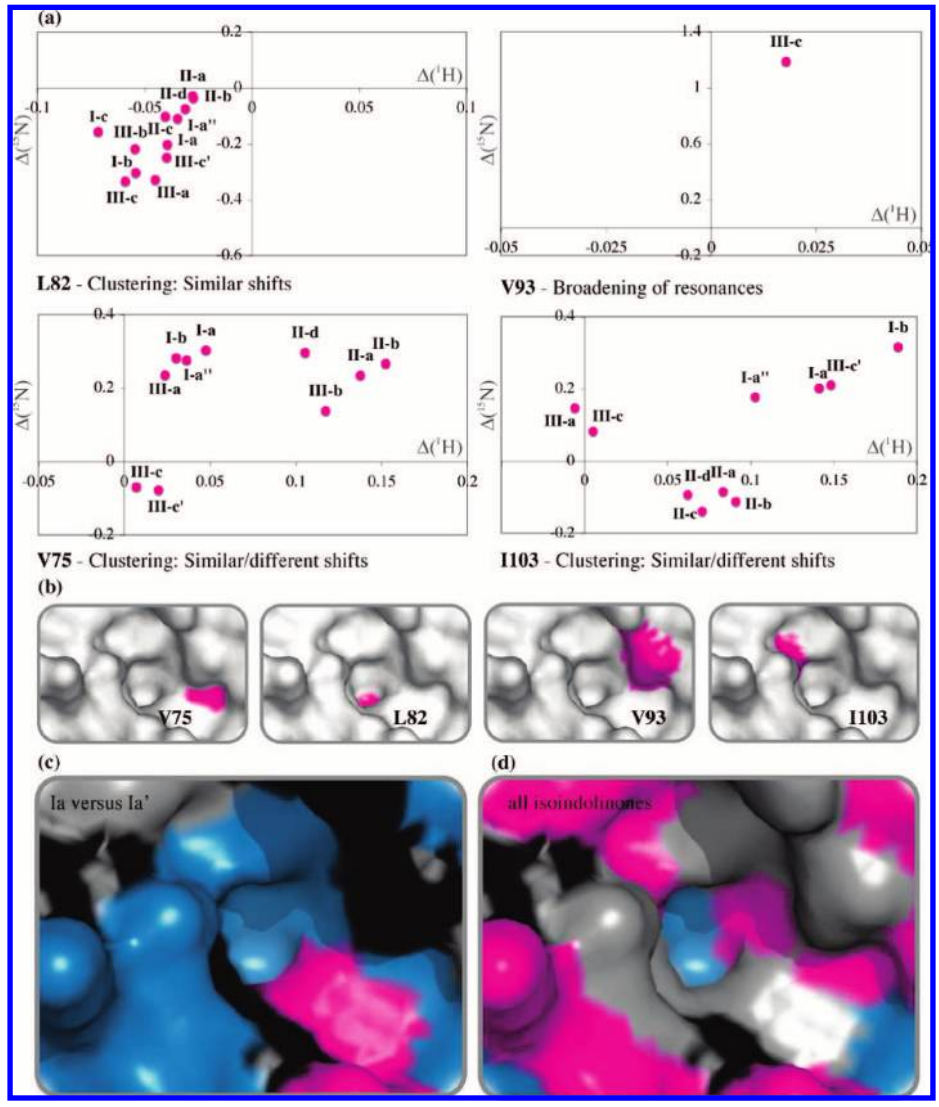

Figure 3. Data analysis. (a) Four examples of "per residue plots", showing the chemical shift of the isoindolinone-bound amino acid. Shifts in the hydrogen dimension are plotted along the X-axis; the Y-axis shows shifts in the nitrogen dimension [ppm]. Depending on the distribution of peaks for structurally related isoindolinones, effects on the chemical environment of each amino acid are considered similar or different. In some cases, migration of peaks could not be traced due to broadening of resonances upon inhibitor binding. (b) Location of each residue presented in (a) in the MDM2 -p53-binding pocket. (c) and (d) Results from chemical shift analysis plotted onto the surface of MDM2. Blue: similarity of chemical shift change, magenta: difference in chemical shift change, gray: broadening for >50% of inhibitors, black: all inhibitors cause broadening of the resonance.

and a clear pattern emerged (Figure 4): for enantiomer 1, a consistent solution between the NMR-derived and GOLD-predicted binding modes could only be found for all inhibitors that did not contain an ether bridge in R′. For enantiomer 2, a consistent solution could only be found for inhibitors containing an ether-bridge in R′. Interestingly, for most binding modes in agreement, the NMR-based docking solution corresponds to the GOLD model with the best energy ranking. The very strong correlation between the NMR-derived models and the top ranked GOLD models suggest strongly that one stereoisomer might indeed be a preferred ligand for MDM2, and that the presence and absence of the ether-group in R′ decides which enantiomer is the better ligand. It is clear that the absence of this ether group greatly limits the conformational flexibility of R′, and these conformational constraints are very likely to affect the binding-mode of these ligands.

Discussion

We have analyzed the perturbation of amide resonances in the hydrophobic cleft of MDM2 by isoindolinone inhibitors. Based on cluster analysis of resonance-frequencies at saturation, we have mapped the effects of inhibitors on each residue according to three categories onto the surface of MDM2 (Figure 3). This allowed easy identification of the location of structurally similar and dissimilar elements for each group of closely related inhibitors.

Comparison of all twelve inhibitors did not indicate areas of similar chemical shift change, suggesting that there is no single binding mode for all inhibitors (Figure 3D). Upon comparison of smaller groups and pairs of inhibitors differing in one structural element, areas with similar and different effects on the resonance frequencies of amides emerged. This allowed localization of the structurally dissimilar element within each group of structurally related inhibitors. For group I and group III, the location of two R-groups (R′ and R″) could be determined. This was achieved through comparison of inhibitors Ia, Ib and Ic to determine the location of R′, and by comparison of Ia to Ia″, revealing the location of R″. Similarly, comparison of IIIa to IIIc allowed localization of R″, and comparison of

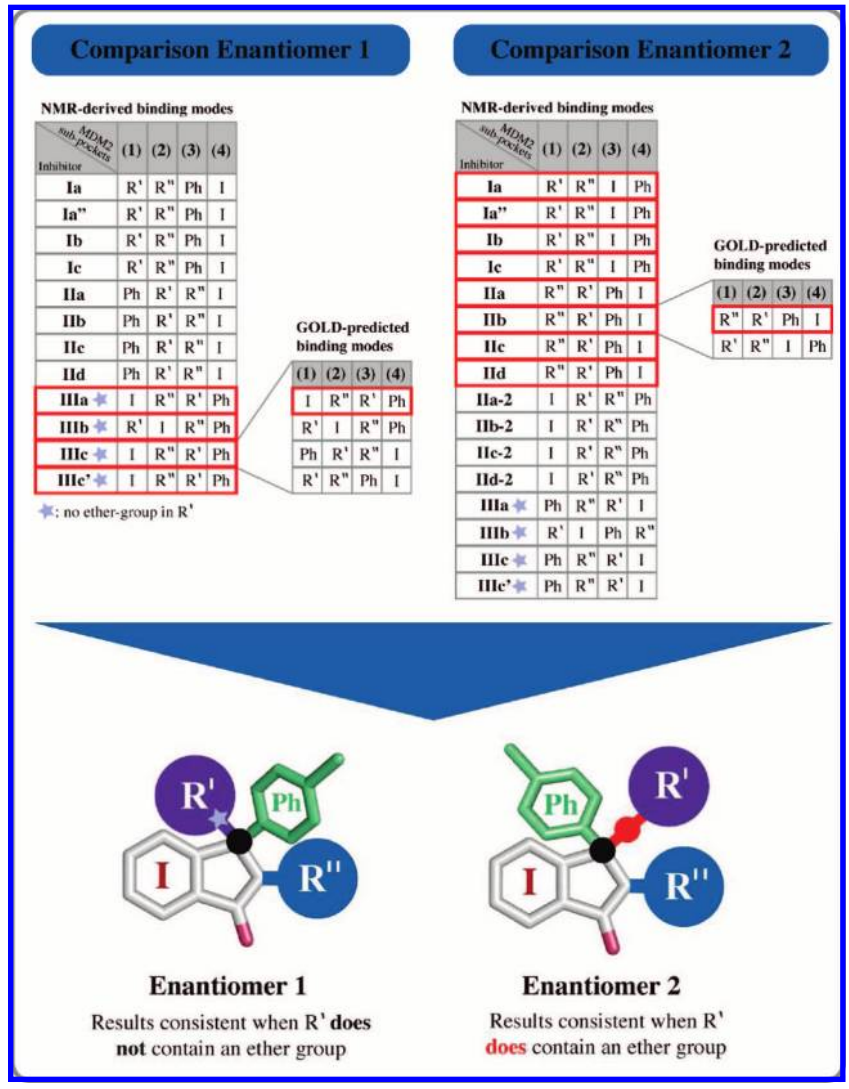

Figure 4. Comparison of NMR-derived binding modes with the models obtained from computational docking. Each line of the table represents one binding mode, i.e. the orientation of the four subgroups of isoindolinones in the 4 subpockets of the MDM2 p53-binding pocket. NMR-derived binding modes for which there was an agreement with the GOLD results are framed in red.

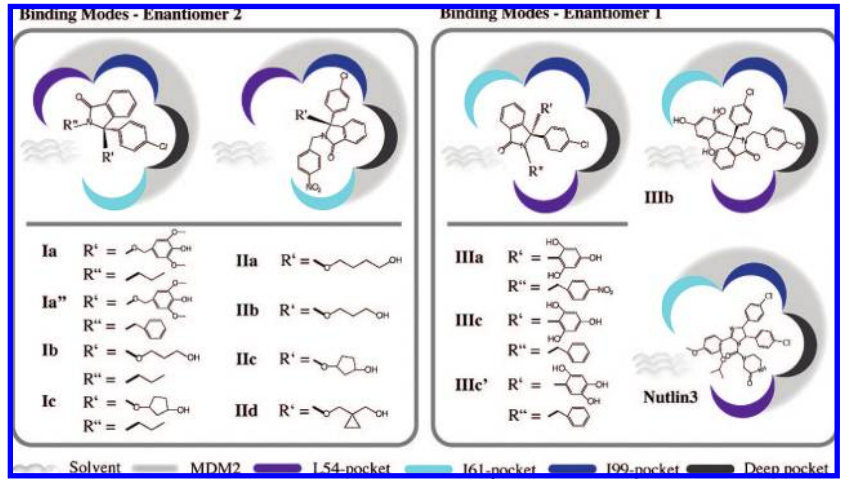

Figure 5. Predicted binding modes of isoindolinones as determined from chemical shift data and molecular docking. Color-coding of subpockets of MDM2 corresponds to Figure 2.

IIIc to IIIc′ revealed the location of R′. The chemical shift perturbations observed for compound IIIb did not correspond to the pattern observed for IIIa and IIIc, respectively, indicating that this compound binds in a different orientation. Compound IIIb contains two halogeno-phenyl groups also present in the Nutlin-scaffold (Figure 3).[11] Comparing the perturbations of IIIb

with chemical shifts induced by Nutlin3 binding to MDM2, similar effects on the Ile99 subpocket and the deep pocket were observed. It was therefore concluded that the chlorophenyl moieties of IIIb bind to MDM2 in a Nutlin-like orientation (data not shown).

The locations of R-groups determined from chemical shift analysis were used for manual docking to explore all possible orientations that are in agreement with the data. In most cases, only one orientation was possible for each enantiomer in three-dimensional space.

Ab initio docking was performed to validate the models of binding obtained from chemical shift analysis. GOLD predicted up to four different binding modes for each of the 24 inhibitors and ranked them according to their energy-score. Upon comparison of these binding-modes with the solutions obtained from chemical shift analysis, distinctive patterns were apparent (Figure 4): for all isoindolinones containing an ether-function in R′, the NMR-derived solution for enantiomer 2 was highly ranked among the GOLD predictions. For all isoindolinones lacking this structural element, the NMR-derived binding mode for enantiomer 1 was present among the GOLD predictions. This supports the binding modes derived from the NMR data, but also suggests that the presence of the ether-group in R′ selects for binding of the enantiomer 2, while enantiomer 1 binds to MDM2 for all molecules in which R′ lacks this functional group. It is plausible that the absence of this ether group has such a marked effect since it affects the overall flexibility of the ligand, otherwise possessing only one rotatable moiety.

For the twelve compounds analyzed here, the data were consistent with four different orientations of binding (summarized in Figure 5). In three cases, a chlorophenyl moiety points into the deep pocket of MDM2, similar to the binding of Nutlins and a benzodiazepinedione.[11,13] In the remaining case, the isoindolinone ring-system points into the deep pocket of MDM2, similar to the Trp23 side-chain of p53.[10] There seems to be a preference for aromatic groups in the Ile99-subpocket, but subpockets Leu54 and Ile61 do not select for a certain type of R-group, such as aryl, alkyl or polar groups.

Conclusions

We have presented a method for determining the orientation of small-molecule ligands in a protein binding-site based on the analysis of magnitude and direction of chemical shift change, exemplified by isoindolinone-binding to MDM2. This method is particularly useful when dealing with low-affinity ligands for which conventional structural methods are not applicable. Furthermore, as this approach is based on the analysis of amide chemical shifts, it is relatively easy to apply. However, one could extend this method by incorporating side-chain chemical shift perturbations to obtain more precise mapping. We have shown that rationalization of chemical shift perturbations induced by a set of structurally related inhibitors is able to reduce the possible orientations of binding significantly. In combination with molecular docking, we obtained a single solution and were able to discern binding of both enantiomers. The binding modes generated here form the basis for further inhibitor design and lead the way to high-affinity candidates for potential clinical investigation.

Acknowledgment. We thank the Wellcome Trust, EPSRC and Cancer Research UK for financial support. The EPSRC Mass Spectrometry Service at the University of Wales (Swansea) is also gratefully acknowledged. We also thank Charles D. Taylor for useful suggestions and carefully reading the manuscript.

Supporting Information Available: Details of inhibitor synthesis; complete refs 13−17 and 24. This material is available free of charge via the Internet at http://pubs.acs.org.

JA8062088